

Contract No:

This document was prepared in conjunction with work accomplished under Contract No. DE-AC09-08SR22470 with the U.S. Department of Energy (DOE) Office of Environmental Management (EM).

Disclaimer:

This work was prepared under an agreement with and funded by the U.S. Government. Neither the U. S. Government or its employees, nor any of its contractors, subcontractors or their employees, makes any express or implied:

- 1) warranty or assumes any legal liability for the accuracy, completeness, or for the use or results of such use of any information, product, or process disclosed; or
- 2) representation that such use or results of such use would not infringe privately owned rights; or
- 3) endorsement or recommendation of any specifically identified commercial product, process, or service.

Any views and opinions of authors expressed in this work do not necessarily state or reflect those of the United States Government, or its contractors, or subcontractors.

February 25, 2020

SRNL-STI-2019-00637, Rev. 0

TO: B. T. BUTCHER, 773-42A
FROM: T. L. DANIELSON, 773-42A
REVIEWER: J. A. DYER, 773-42A

COMPARISON OF SLIT TRENCH AND ENGINEERED TRENCH 3D VADOSE ZONE CONCEPTUAL MODELS

Summary

In the next revision of the E-Area Low-Level Waste Facility (ELLWF) Performance Assessment (PA), radionuclide groundwater transport from slit (ST) and engineered trenches (ET) will be simulated using 3-dimensional PORFLOW (ACRi, 2010) models representing the vadose zone. In total, the conceptual framework will aim to model 29 total trenches with a degree of conservatism that provides a high level of confidence in meeting performance objectives. The implementation of generic conceptual models allows for a reasonable number of simulation scenarios, thereby reducing the chances of errors and enabling a better one-to-one comparison between the results, while still capturing the most important features of each trench. The current investigation seeks to understand if a generic trench model based on the general ET footprint can justifiably be used for representing both STs and ETs while maintaining a reasonable degree of conservatism. In this process, the groundwater transport of several key radionuclides was simulated for both ET and ST geometries and the flux-to-the-water-table profiles were compared. For all radionuclides simulated, the ET geometry is shown to be conservative (i.e., produces the highest peak flux to the water table).

Model Geometry

The generic model implementation of the ET and ST geometries, which is presumed to be a close representation of the models to be used in the next revision of the ELLWF PA, is shown in Figure 1 through Figure 5. The same mesh was used for both the ET and ST simulations so that numerical differences caused by spatial discretization are kept negligible – only material properties were changed for the appropriate regions for each of the trenches (e.g., regions between trench segments in the ST). The interim and final covers are assumed to extend across the entire model domain in the y-direction and have a 10-foot and 40-foot overhang, respectively, from the edge of the trench footprint in the x-direction. The dimensions of the specific material features for each model are provided in Table 1.

We put science to work.™

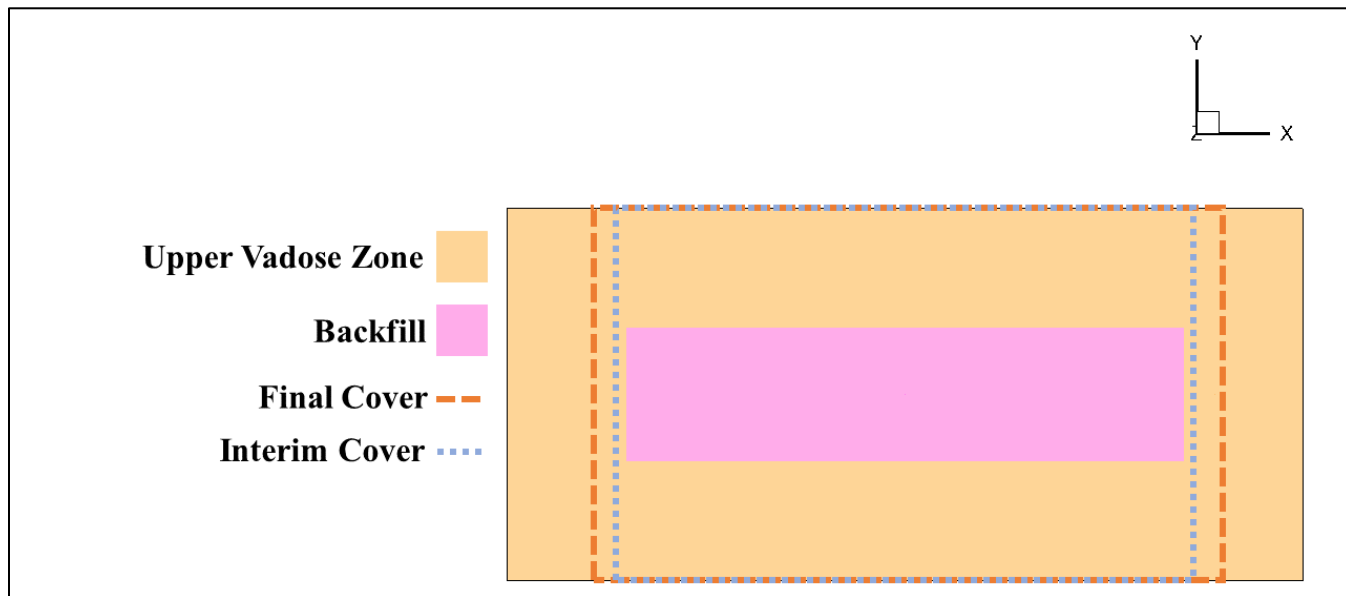


Figure 1. Cross-section of the engineered trench geometry in the XY plane

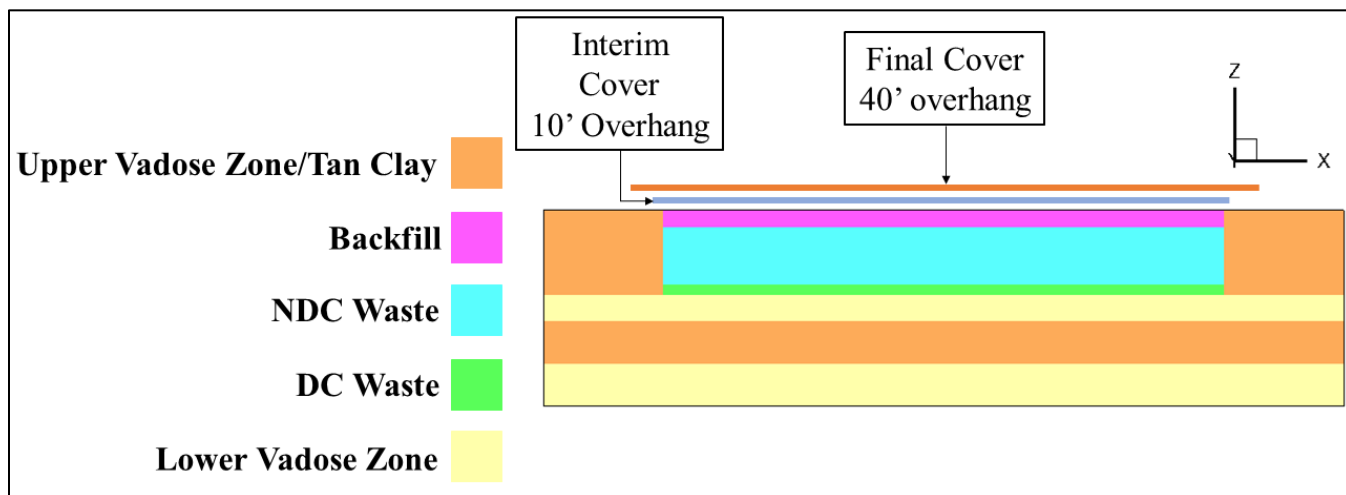


Figure 2. Cross-section of the engineered trench and slit trench geometry in the XZ plane

We put science to work.™

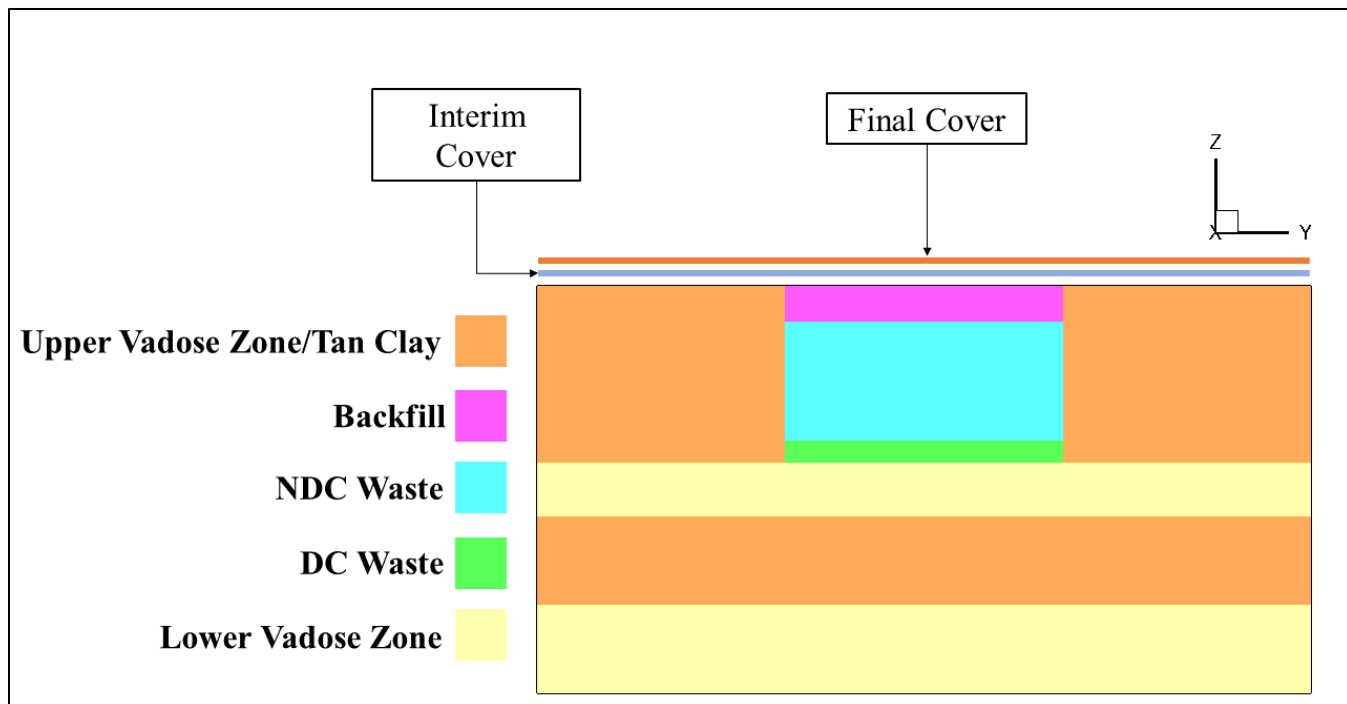


Figure 3. Cross-section of the engineered trench geometry in the YZ plane

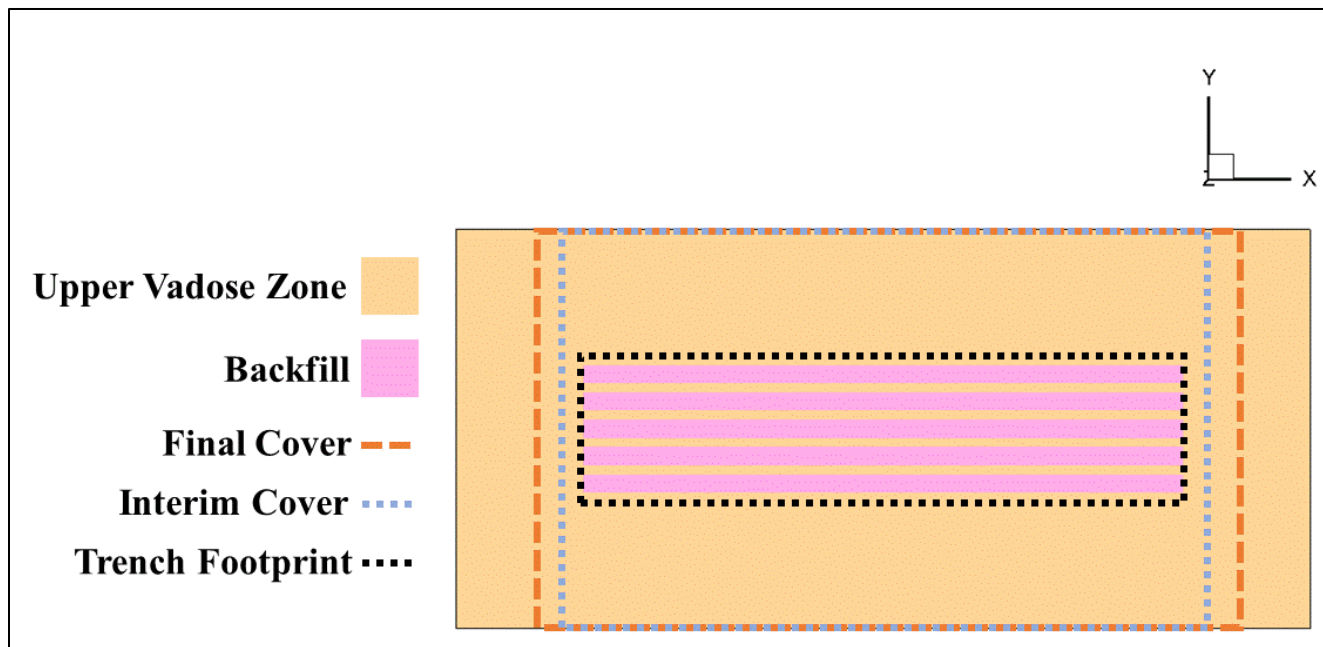


Figure 4. Cross-section of the slit trench geometry in the XY plane

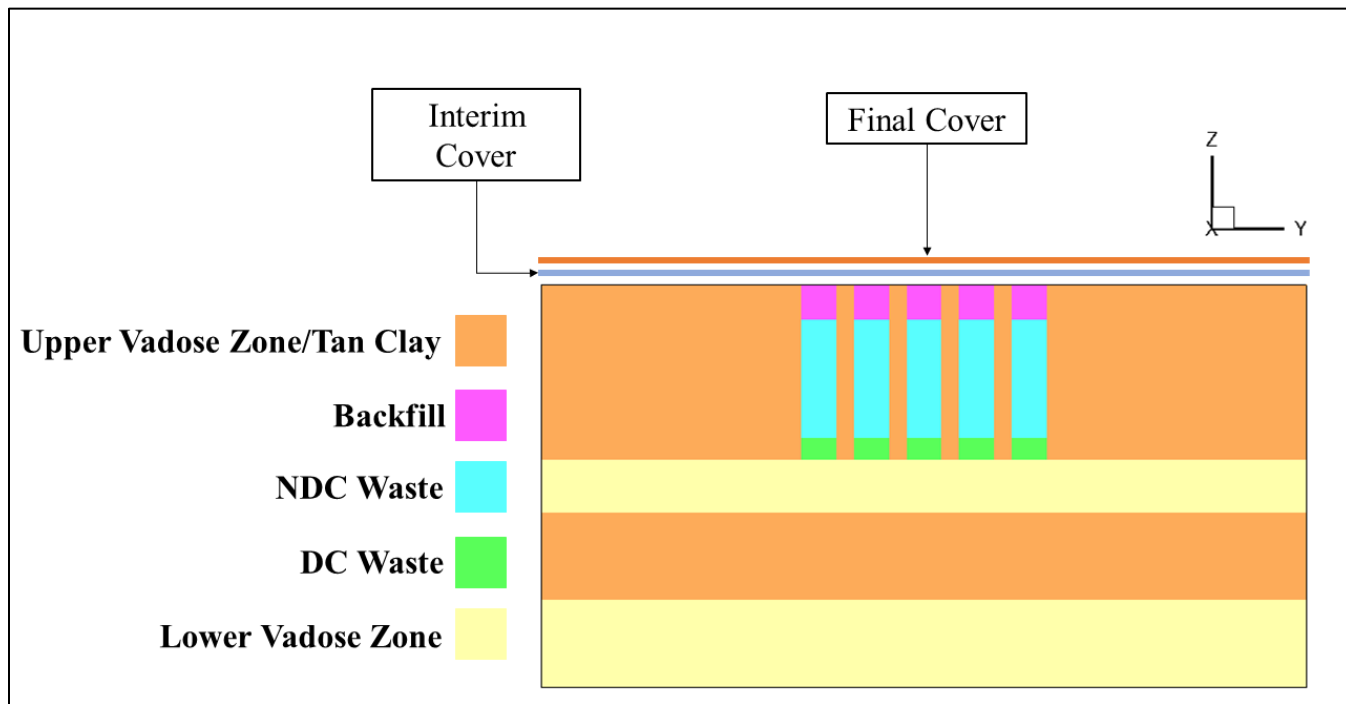


Figure 5. Cross-section of the slit trench geometry in the YZ plane

We put science to work.™

Table 1. Key dimensions of slit and engineered trench geometries in x, y, and z directions

Description	Dimensions
<i>Upper Vadose Zone</i>	936' x 437' x 20'
<i>ET Backfill</i>	656' x 157' x 4'
<i>ST Backfill (Individual Segment)</i>	656' x 20' x 4'
<i>ET NDC Waste</i>	656' x 157' x 13.5'
<i>ST NDC Waste (Individual Segment)</i>	656' x 20' x 13.5'
<i>ET DC Waste</i>	656' x 157' x 2.5'
<i>ST DC Waste (Individual Segment)</i>	656' x 20' x 2.5'
<i>ST Footprint</i>	656' x 157' x 20'
<i>Upper Vadose Zone between ST segments</i>	656' x 10' x 20'
<i>Lower Vadose Zone between Tan Clay and Upper Vadose Zone</i>	936' x 437' x 6'
<i>Tan Clay</i>	936' x 437' x 10'
<i>Lower Vadose Zone beneath Tan Clay</i>	936' x 437' x 10'

Timeline, Material Properties, and Boundary Conditions

The standard PORFLOW vadose zone modeling workflow was followed, where a series of 74 steady-state flow fields (the same ET02 timeline used by Hamm et al., 2018) were computed to be used as inputs for transient radionuclide transport simulations. The same timeline was used for both trench types which accounts for the placement of waste and the application/degradation of the various trench covers. In the current work, an interim and final cover are applied at Year 46 and 171, respectively. During radionuclide transport simulations, 1 Ci of waste is assumed to be uniformly distributed in the waste zone(s). At Year 171, along with the application of the final cover, dynamic compaction is assumed to occur which transfers the waste from the 16-foot total height of the ‘DC Waste’ + ‘NDC Waste’ zones to the 2.5-foot ‘DC Waste’ zone. This waste transfer is accompanied by a change in the material properties, where the ‘Backfill’ material zone shifts from ‘OSC Before’ to ‘OSC After,’ the ‘NDC Waste’ zone shifts from ‘ET Boxes Before’ to ‘OSC After,’ and the ‘DC Waste’ zone shifts from ‘ET Boxes Before’ to ‘ET Boxes After.’ All other material properties remain the same throughout the simulation (see Nichols, 2020 for more detail on material properties).

The boundary conditions are applied for two separate cases: 1) intact and 2) subsided (slope-length-weighted, cap-averaged infiltration rate), which were taken directly from Case01 and Case11a used in the 2018 Special Analysis (Hamm et al, 2018). A discrete-hole subsided case was not considered because several assumptions would be required to account for the spatial distribution of subsided holes given the substantial differences between the two trench geometries. The complexities associated with adequately modeling discrete, subsided holes are a prime motivator for the adoption of a generic trench model based

on the ET geometry. The intact, subsided, and background (four-foot-thick operational soil cover) infiltration rates are shown in Table 2. For portions of the geometry not impacted by either cover, the background infiltration rate is applied across the entire timeline. The subsided infiltration rate is applied only over portions of the geometry corresponding to the trench or trench segments (i.e., overhangs and locations between trench segments are considered intact through time).

Results

Figure 6 through Figure 9 show the saturation profiles for the ET and ST geometries at the end of the institutional control period (i.e., the first time interval when the final closure cap is applied) for the intact and subsided cases in the XZ- and YZ-planes. Note the variability in the saturation profile for the ST compared to the uniformity of the saturation profile for the ET as shown especially in Figure 7 and Figure 9. The saturation profiles in the XZ-planes are qualitatively very similar for both trench geometries with only a slightly higher overall saturation in the trench segments than is shown in the ET. Likewise, the ST geometry has slightly higher saturation values in the vadose zone beneath the trench than the ET.

The 74 flow fields were utilized in transient radionuclide transport simulations for six radionuclides: C-14, H-3, I-129, Sr-90, Tc-99, and U-235. These six radionuclides were chosen because the ranges in their values for K_d and half-life should largely capture all relevant groundwater transport behavior that manifests from the range of radionuclide properties (e.g., low K_d + long half-life, high K_d + long half-life, low K_d + short half-life, etc.). The flux-to-the-water-table profiles for each of the six radionuclides are shown in Figure 10 through Figure 15. Not surprisingly, based on similarities in the saturation profiles, the time-dependent flux to the water table for the intact case is nearly identical for all radionuclides between the two trench geometries. A comparison of the subsided cases, however, shows that the ET geometry is the more conservative implementation, as the peak flux to the water table is higher for all radionuclides tested. There are two phenomena responsible for this result. First, the flux-to-the-water-table profiles show that the ST geometry results in slightly higher fluxes than the ET geometry during the earlier time periods (i.e., before the peak occurs), thereby reducing the peak later in time. Second, the concentration profiles in Figure 16 show that the clayey material separating ST segments acts to delay the release of radionuclides through time. This is primarily a result of dynamic compaction occurring only in the waste zone. Following dynamic compaction, some residual radionuclides remain trapped well above the 2.5-foot final thickness of the dynamically compacted waste zone. Although the radionuclide concentrations appear to be small in the concentration cross-sections, the intermediate clayey regions that are not dynamically compacted comprise approximately 36% of the overall 157 x 656 ft² trench footprint

Table 2. Intact and subsided infiltration rates

Year	Intact Infiltration Rate (in/yr)	Subsided Infiltration Rate (in/yr)
0 (Background)	15.78	15.78
46	0.1	0.1
171	0.00088	5.8578
251	0.00791	5.824
361	0.18881	5.938
371	0.2041	5.972
411	0.32	6.02
451	0.41	6.092
551	1.46	6.771
731	3.23	7.928
1171	7.01	10.38

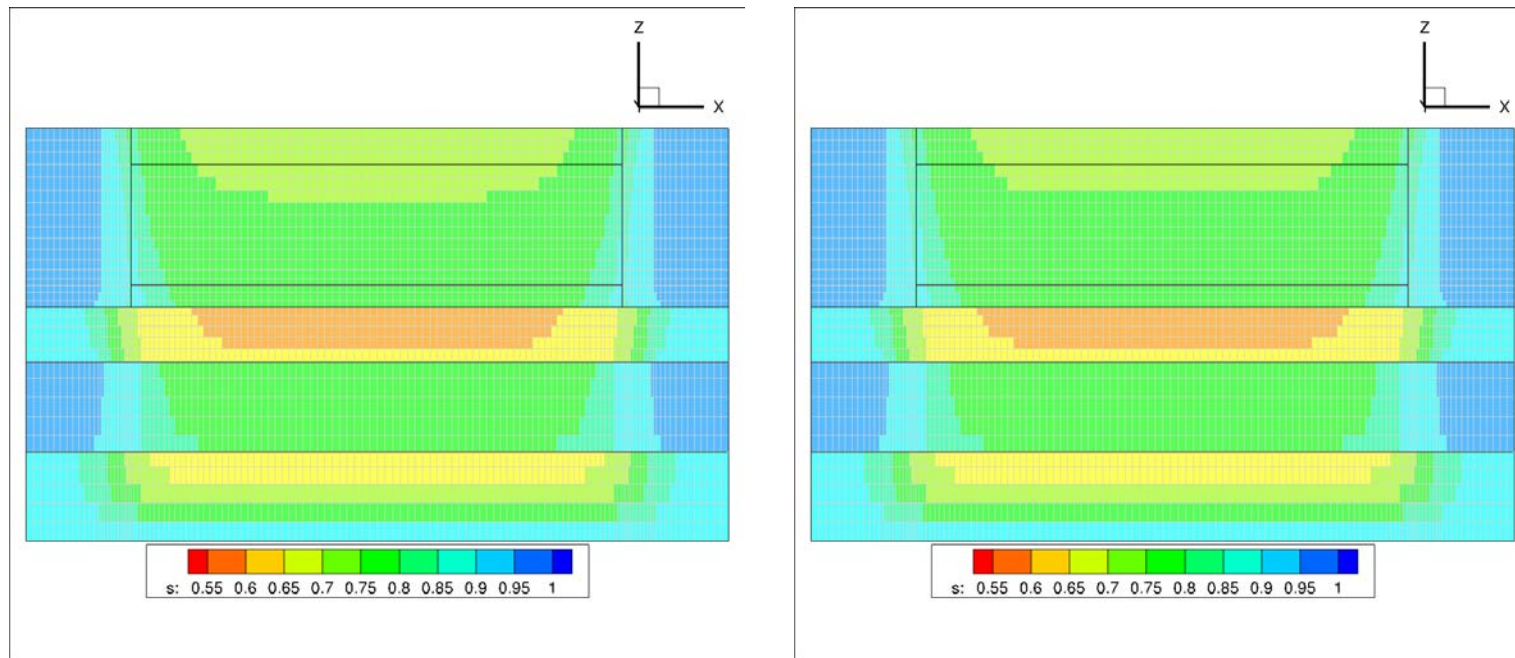


Figure 6. Saturation profile in an XZ-plane for the ET (left) and ST (right) intact case at the end of institutional control

We put science to work.™

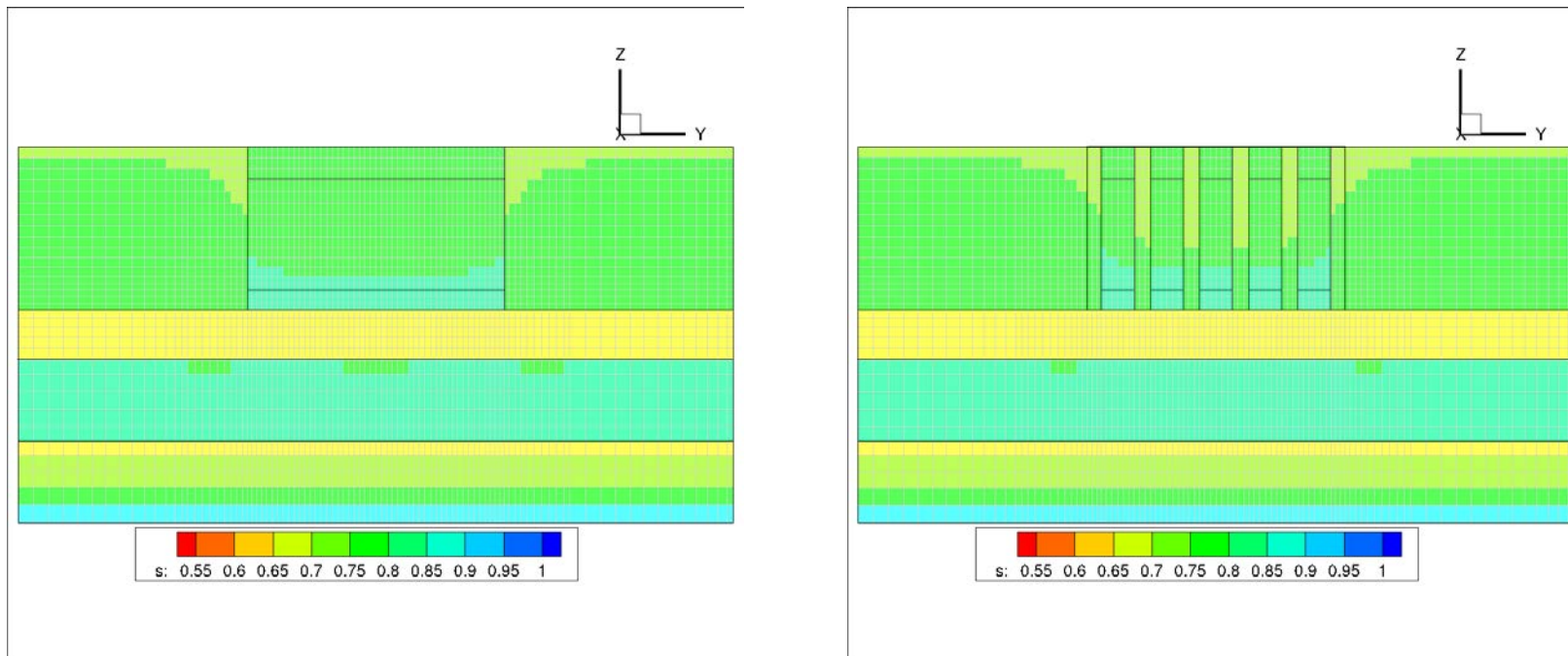


Figure 7. Saturation profile in an YZ-plane for the ET (left) and ST (right) intact case at the end of institutional control

We put science to work.™

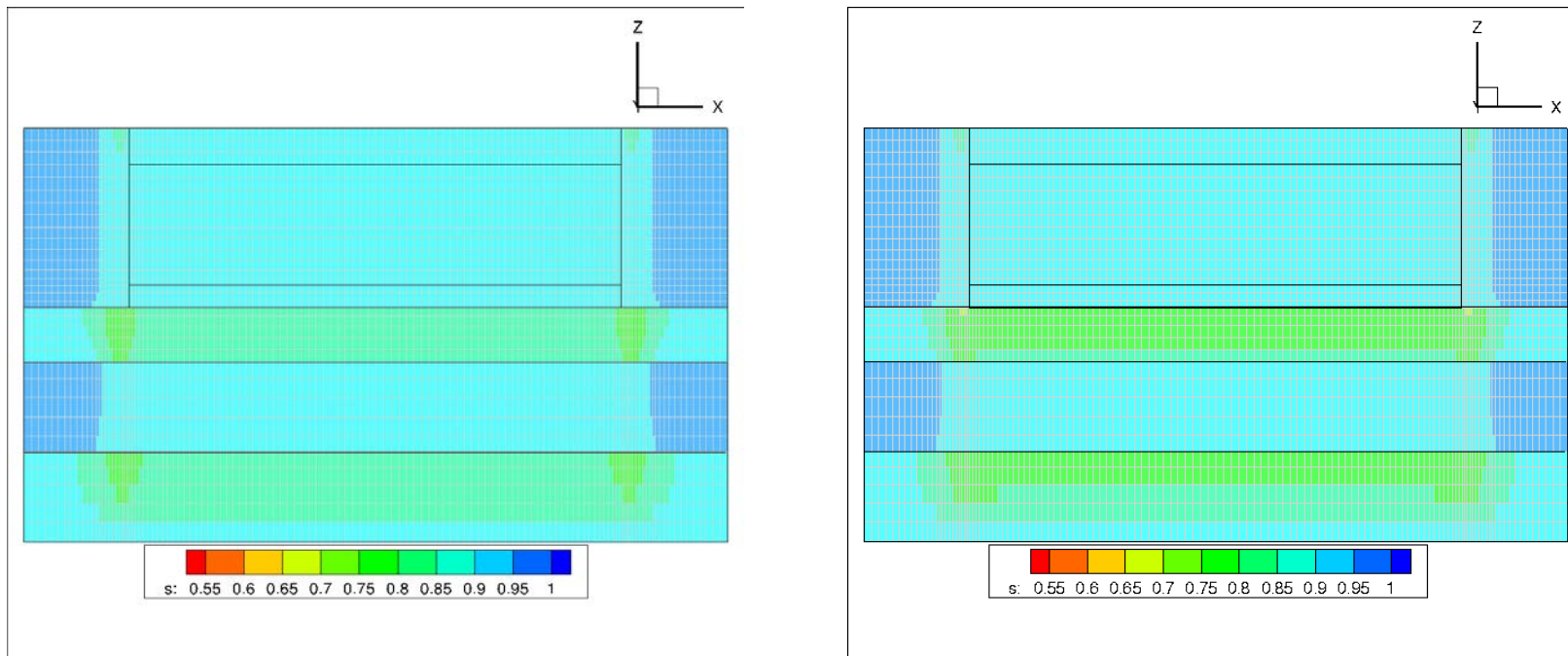


Figure 8. Saturation profile in an XZ-plane for the ET (left) and ST (right) subsided case at the end of institutional control

We put science to work.™

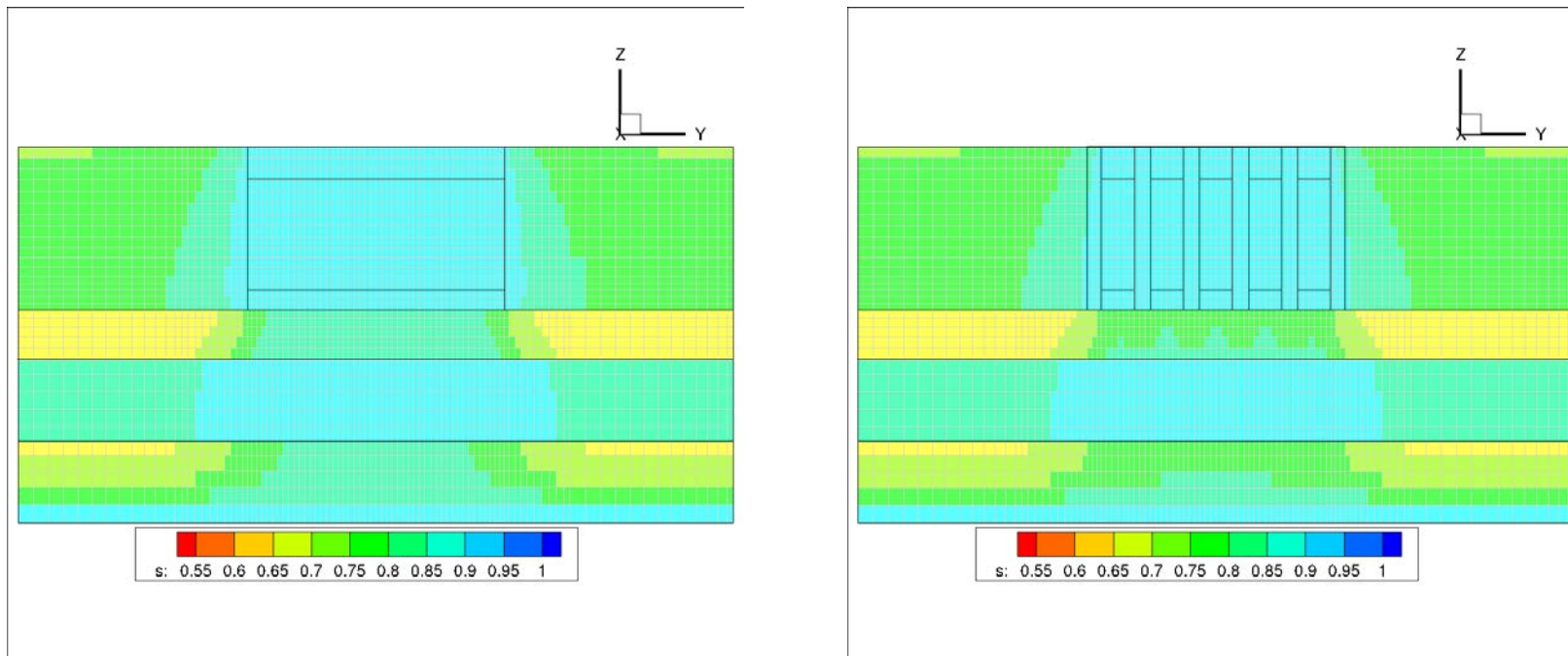


Figure 9. Saturation profile in an YZ-plane for the ET (left) and ST (right) subsided case at the end of institutional control

We put science to work.™

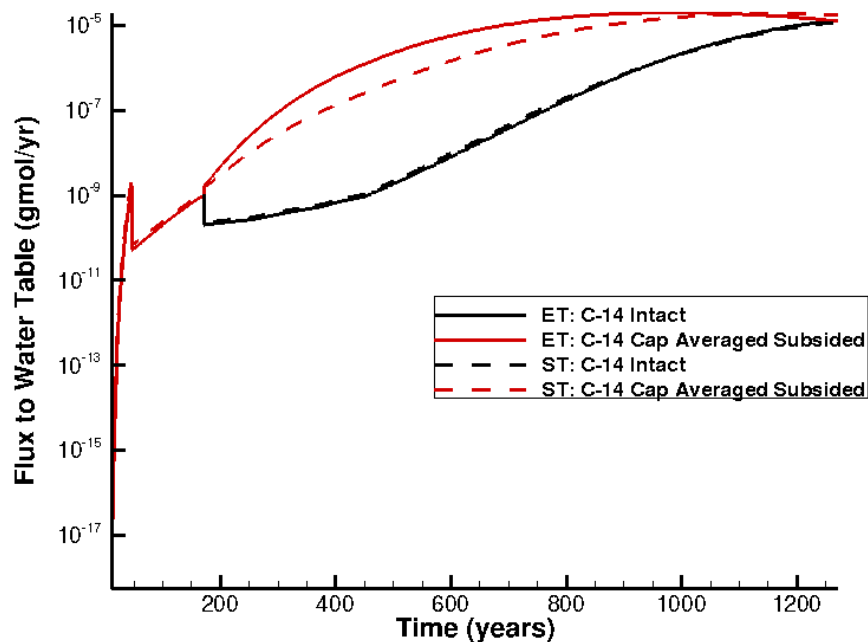


Figure 10. Flux-to-the-water-table profile, C-14

We put science to work.™

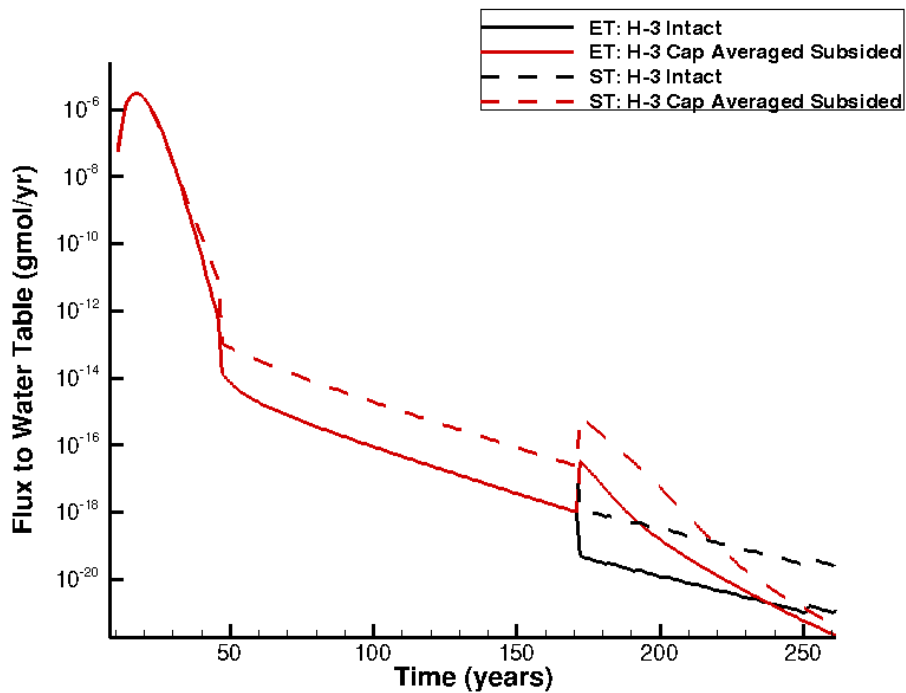


Figure 11. Flux-to-the-water-table profile, H-3

We put science to work.™

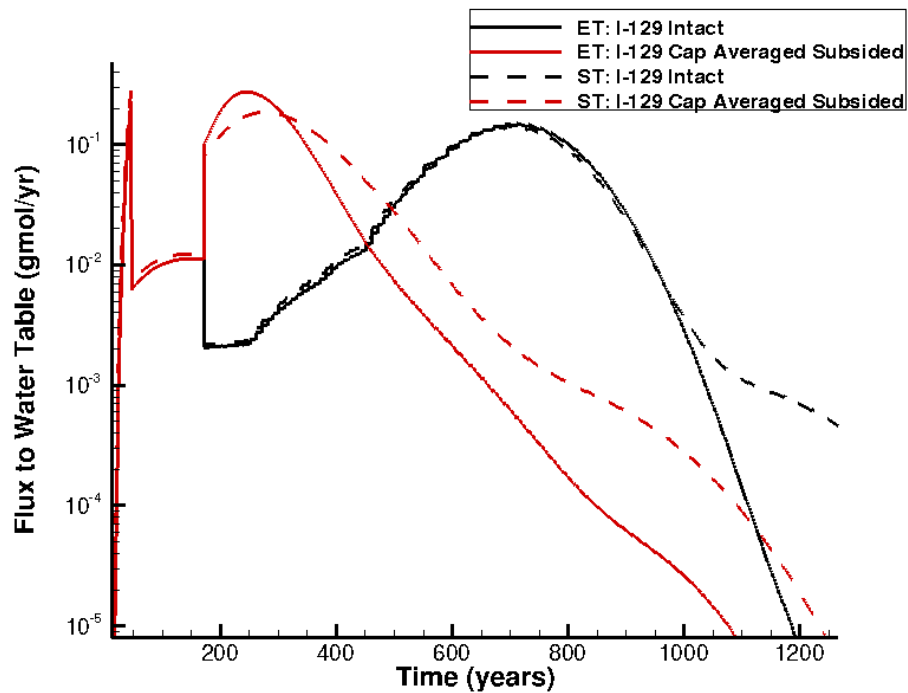


Figure 12. Flux-to-the-water-table profile, I-129

We put science to work.™

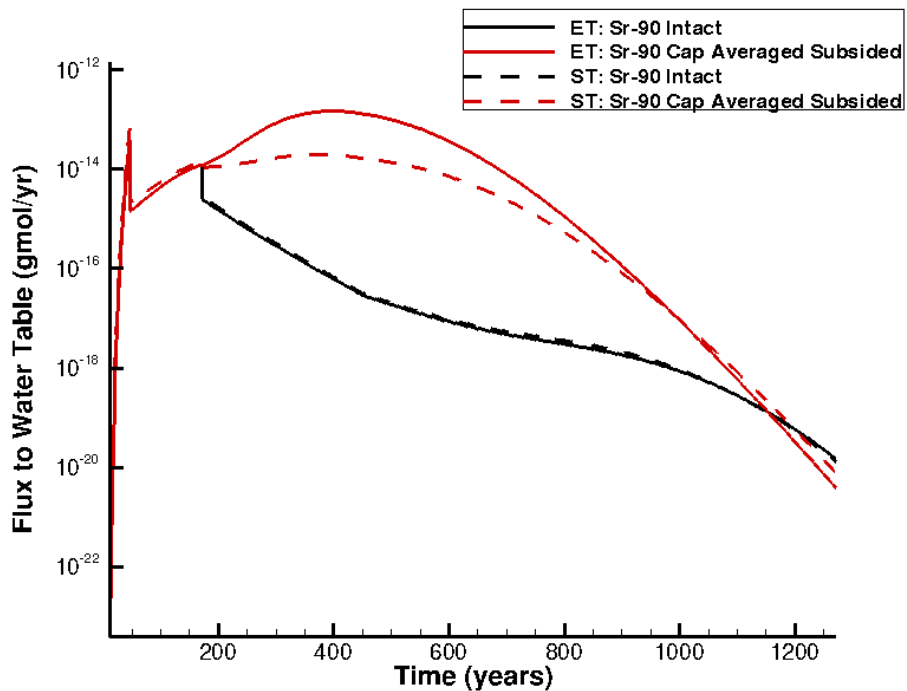


Figure 13. Flux-to-the-water-table profile, Sr-90

We put science to work.™

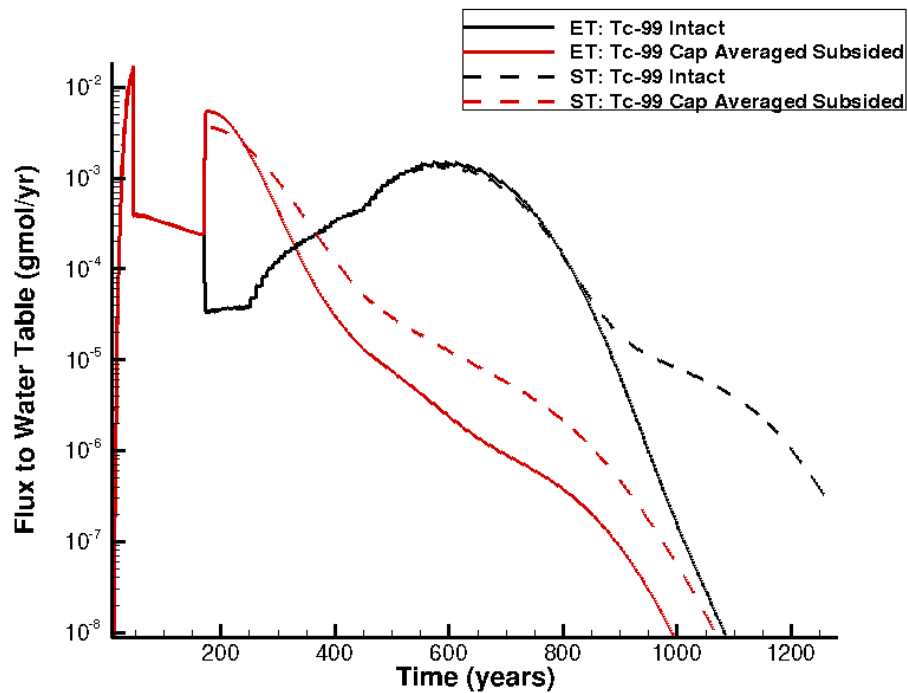


Figure 14. Flux-to-the-water-table profile, Tc-99

We put science to work.™

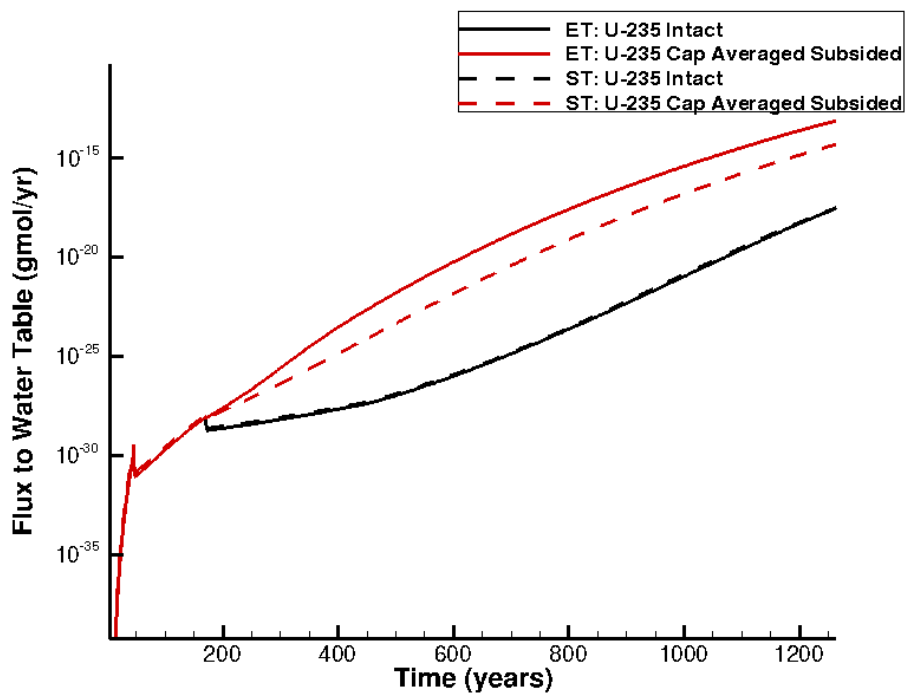
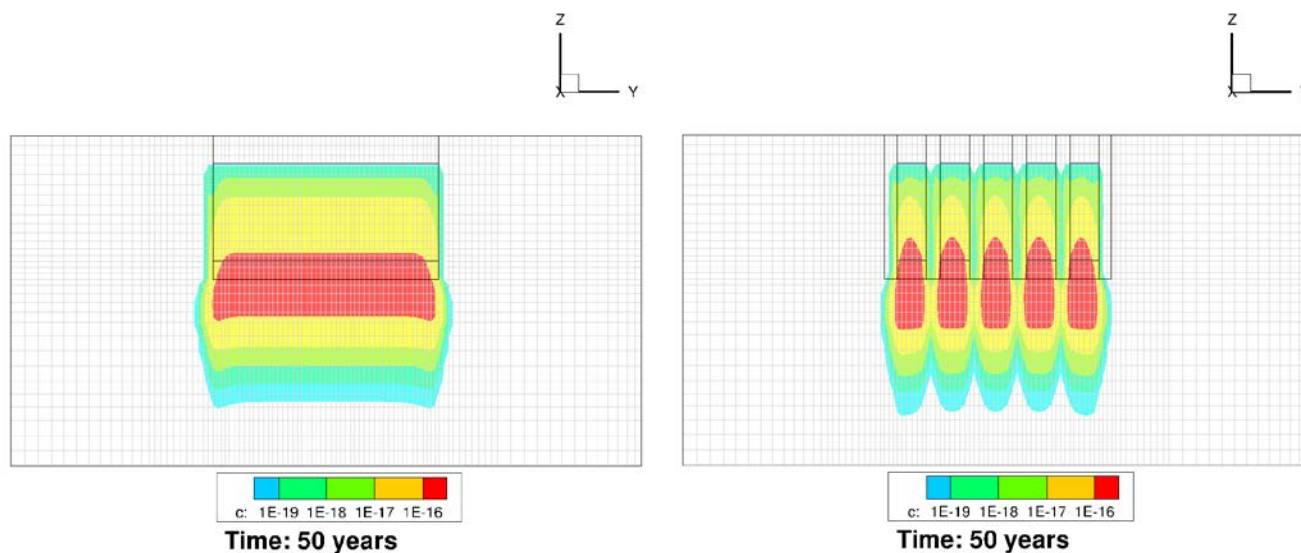


Figure 15. Flux-to-the-water-table profile, U-235



We put science to work.™

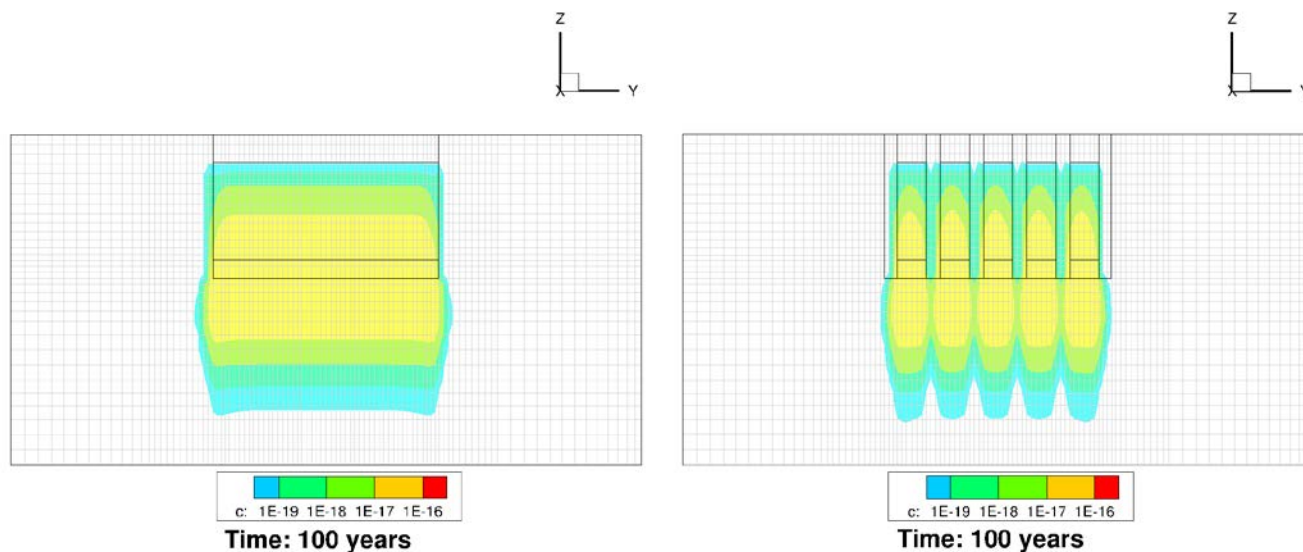
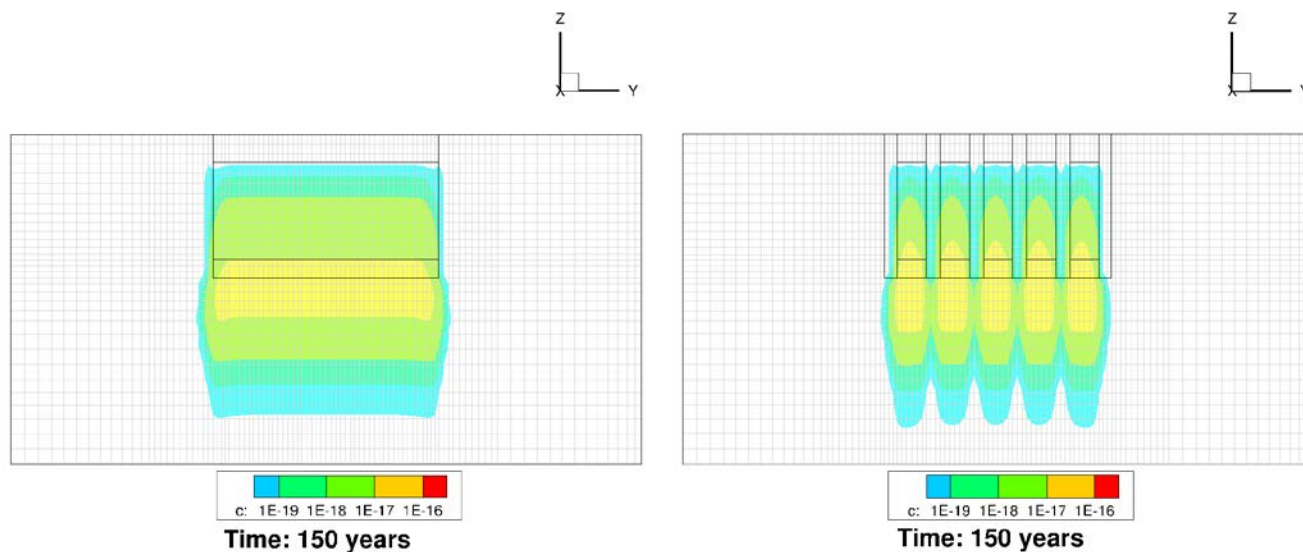


Figure 16. Comparison of Sr-90 concentration profile at 50-year time intervals for the ET (left) and ST (right) geometries



We put science to work.™

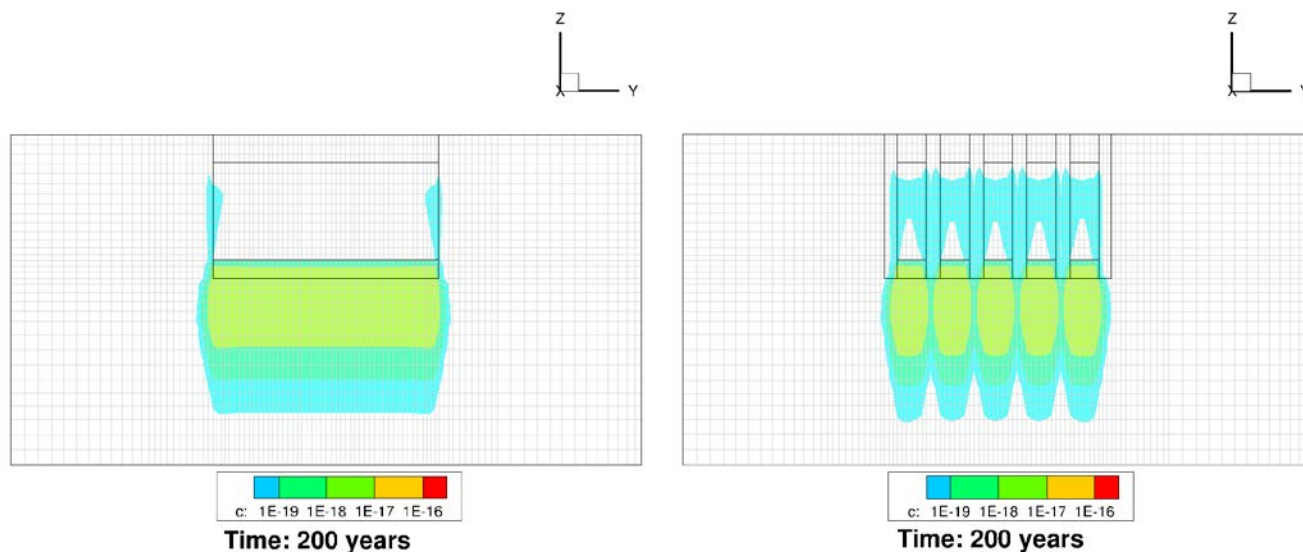
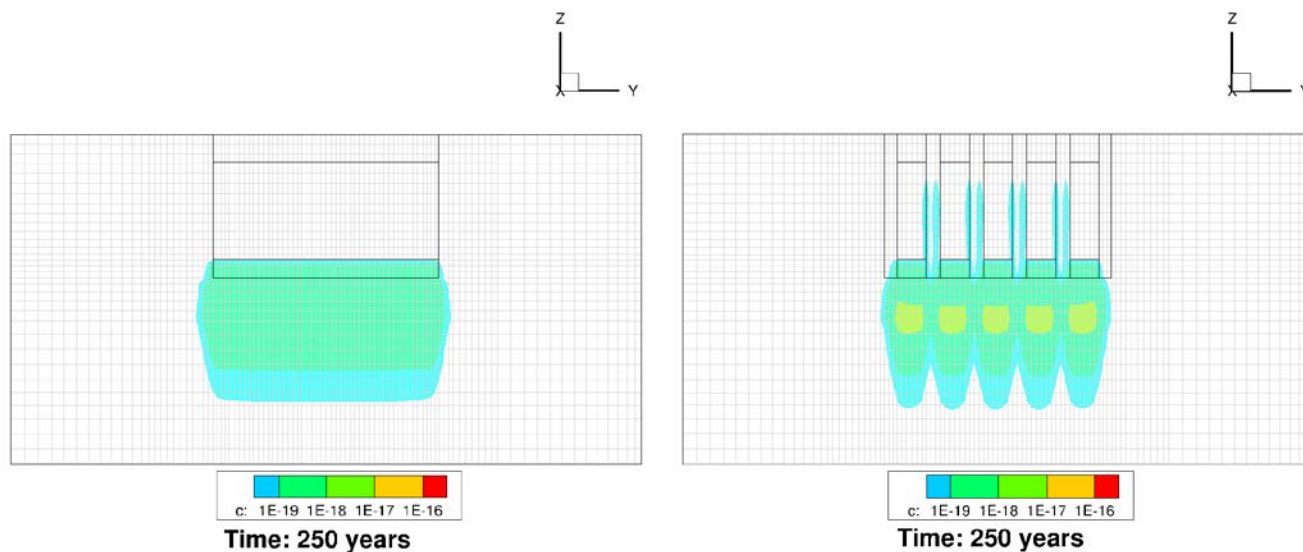


Figure 16 (cont'd). Comparison of Sr-90 concentration profile at 50-year time intervals for the ET (left) and ST (right) geometries



We put science to work.™

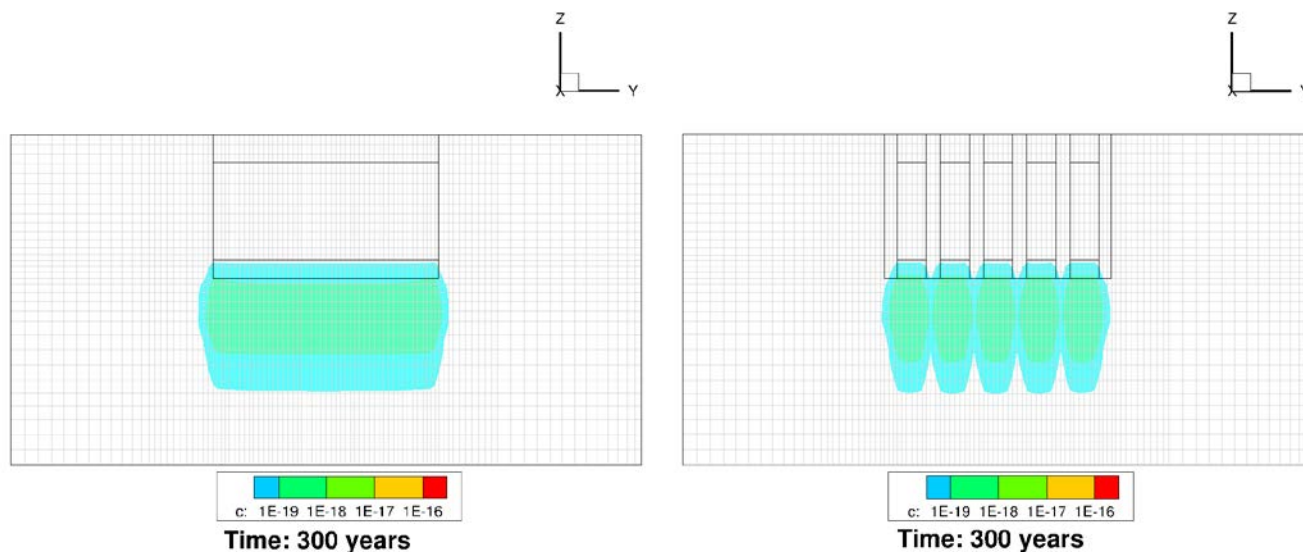
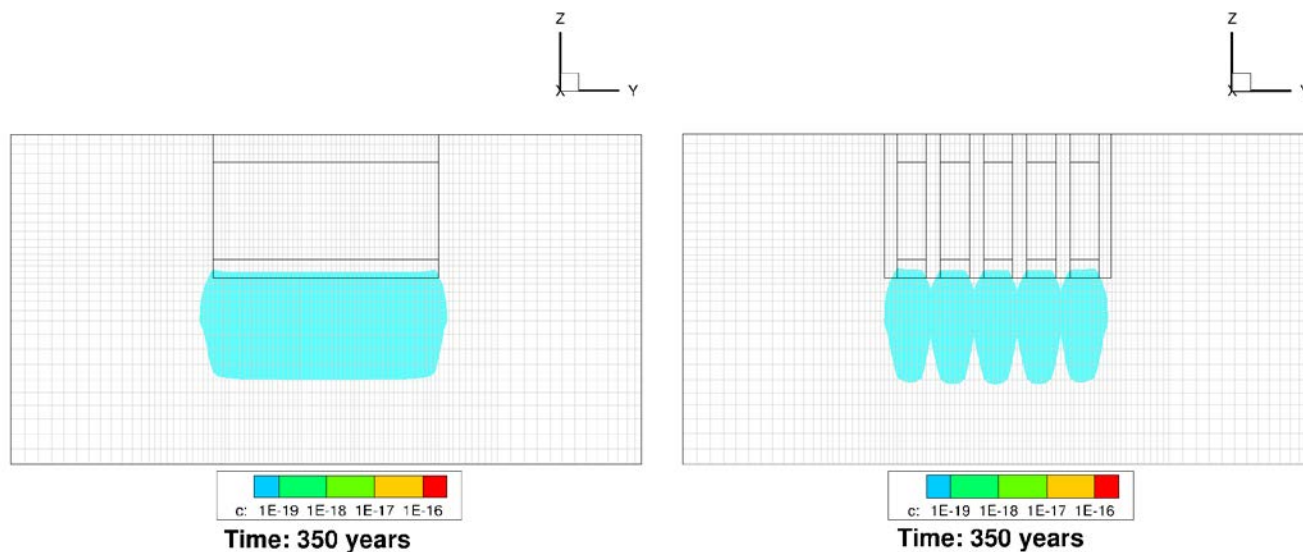


Figure 16 (cont'd). Comparison of Sr-90 concentration profile at 50-year time intervals for the ET (left) and ST (right) geometries



We put science to work.™

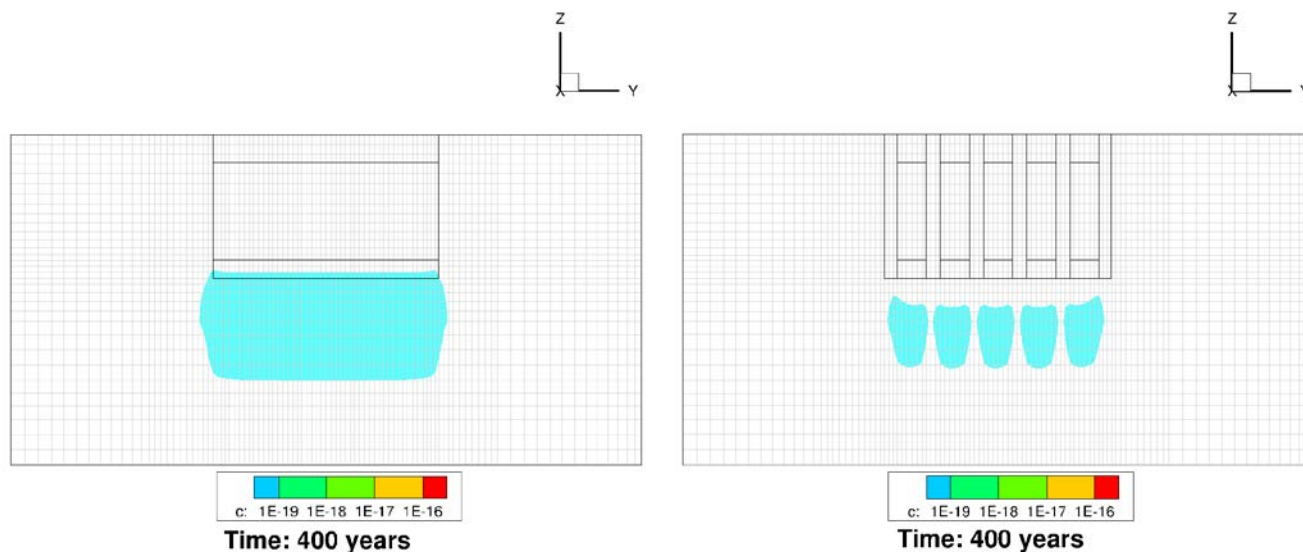


Figure 16 (cont'd). Comparison of Sr-90 concentration profile at 50-year time intervals for the ET (left) and ST (right) geometries

We put science to work.™

References

ACRi (2018) PORFLOW User's Manual, *Keyword Commands Version 6.42.9, Revision 0*. Analytical & Computational Research, Inc., Los Angeles, CA, April 23, 2018.

Hamm, L. L., Aleman, S. E., Danielson, T. L., and Butcher, B.T. (2018) Unreviewed Disposal Question Evaluation: Impact of Updated GSA Flow Model on E-Area Low-Level Waste Facility Groundwater Performance. SRNL-STI-2018-00624, Rev. 0. Savannah River National Laboratory, Aiken, SC.

Nichols, R. L. (2020) Hydraulic Properties Data Package for the E-Area Soils, Cementitious Materials, and Waste Zones Update. SRNL-STI-2019-00355. Savannah River National Laboratory, Aiken, SC.

Distribution List

S. E. Aleman, 735-A	T. Hang, 773-42A
C. J. Bannochie, 773-42A	C. C. Herman, 773-A
B. T. Butcher, 773-42A	D. G. Jackson, 773-42A
D. A. Crowley, 773-42A	R. L. Nichols, 773-42A
T. L. Danielson, 773-42A	F. G. Smith, 773-42A
K. L. Dixon, 773-42A	J. L. Wohlwend, 773-42A
J. A. Dyer, 773-42A	T. N. Foster, EM File, 773-42A – Rm. 243
A. P. Fellingner, 773-42A	Records Management (EDWS)
L. L. Hamm, 735-A	

We put science to work.™